



Experimental Study on Strengthening of Corroded RC Beams with High-Performance Steel Fiber Mortar and Normal Reinforcements

Thanh-Hung Nguyen¹ · Dinh-Hung Nguyen² · Duy-Duan Nguyen³

Received: 8 July 2021 / Revised: 28 September 2021 / Accepted: 13 November 2021 / Published online: 1 December 2021
© Iran University of Science and Technology 2021

Abstract

This study evaluated the performance of corroded reinforced concrete (RC) beams strengthened with high-performance steel fiber mortar and normal reinforcements. For that, six RC beams were corrosively imposed in 1 month, 2 months, and 3 months with a 3% NaCl solution and the direct current power type of $900 \mu\text{A}/\text{cm}^2$. As a result, the weight reduction of reinforcements of the beams due to three corrosion levels was 11.3%, 14.3%, and 24.8%, respectively. Those corroded beams were thereafter strengthened using the high-performance steel fiber mortar and normal reinforcements. A series of flexural tests were conducted to quantify the structural capacity improvement of strengthened RC beams. The experimental results showed that the stiffness, strength, and ductility of the strengthened beams were significantly higher than those of the corroded and non-corroded RC beams. Additionally, the strengths of the retrofitted beams were almost similar, and it was approximately 2.35 times and 2.52 times larger than that of the non-corroded and corroded RC beams, respectively. The high-performance steel fiber mortar can be a feasible solution for the strengthening of corroded or degraded RC structures. Moreover, the damage indicators of the tested beams, which are crack patterns, crack width evolution, and strain distribution of reinforcing bars, were further analyzed in this study.

Keywords Reinforced concrete beam · Corrosion · Strengthening · High-performance steel fiber mortar · Flexural capacity

1 Introduction

Reinforced concrete (RC) structures have been predominantly constructed around the world. Usually, infrastructures are designed with a certain lifespan. However, after a period of operation, the structural members of RC structures are degraded due to the effects of load factors and environmental conditions [1]. Specifically, the corrosion of

reinforcement in RC structures located near the coastline is shown to be very high. Accordingly, the load-bearing capacity and service life of structures are reduced compared to the pristine condition. Consideration of the effects of degradation of materials on the structural capacity of RC members is necessary, especially due to corrosion of reinforcement.

Previously, numerous studies investigated the structural behaviors of RC beams and columns strengthened with different methods. Steel jacket, a conventional technique, has been commonly applied for retrofitting of RC columns [2] and beams [3–5]. They demonstrated that steel jackets can considerably improve the strength and load-carrying capacity of structural members. In addition to steel jackets, concrete and RC jackets have also been used as preferable solutions in many last decades, in which both strength and ductility of RC cross-sections were significantly enhanced. Vandoros and Dritsos [6] proved the positive effects of concrete jackets on the strength and stiffness of RC columns. Campione et al. [7] also highlighted the importance of reinforced concrete jackets on improving the strength

✉ Duy-Duan Nguyen
duyduankxd@vinhuni.edu.vn

Thanh-Hung Nguyen
nthung@hcmute.edu.vn

Dinh-Hung Nguyen
ndinhhung@hcmiu.edu.vn

¹ Department of Civil Engineering, Ho Chi Minh University of Technology and Education, Ho Chi Minh, Vietnam

² International University-HCM National University, Ho Chi Minh, Vietnam

³ Department of Civil Engineering, Vinh University, Vinh 461010, Vietnam

and deformation of RC columns noticeably. Furthermore, systematic consideration of the interfacial slip effects in analyzing jacked RC beams was conducted by Alhadid and Youssef [8]. The advantages of the retrofitted technique were demonstrated, however the deterioration of structures due to corrosion was not considered in the strengthening procedure of those studies.

Several retrofitting methods using advanced materials have been employed for RC members in recent times, in which textile-reinforced mortar (TRM) and fiber-reinforced polymer (FRP) are common solutions. Textile-reinforced mortar was normally applied for the shear strengthening of RC beams [9–12]. Experimental results showed that the shear resistance was substantially gained and a transformation shear failure to flexural failure was made if sufficient TRM layers were used. Meanwhile, the RC structures strengthened with FRP demonstrated a significant improvement of ductility, flexural and shear strength, as well as durability [13–16]. Additionally, the FRP jackets were applied for retrofitting of corroded RC beams [17–19]. This technique reduced the retrofitted time and required a simple process. However, there are some limitations such as debonding at the FRP-concrete interface and repair cost.

Concrete is a brittle and low tensile strength material. The new product, created by adding small steel fibers and silica fume into a cementitious/concrete matrix, is known as a high-performance fiber reinforced composite. This material can improve the compressive and tensile strength, flexural strength, crack evolution, and load-bearing capacity of structural components [20]. Additionally, in the study of Shah and Naaman [21], they pointed out that the tensile/flexural strength of steel fiber-reinforced mortar was 2–3 times larger than that of plain mortar specimens. Due to its ease of application, fiber reinforced concrete/mortar has been also employed to strengthen the load-carrying capacities of flexural members [22].

The strengthening method using fiber reinforced concrete or cement for RC and masonry structures has been utilized in recent years [23–27]. Martinola et al. [28] investigated the effects of fiber reinforced concrete (FRC) jackets on behaviors of strengthening RC beams using both experimental and numerical methods. They emphasized that FRC significantly affected ultimate and serviceability limit states. Ruano et al. [29] experimentally evaluated the performance of RC beams retrofitted with steel FRC. The results showed that the strengthened beams exhibited a notable increment of strength and deformation capacity. Specifically, Lampropoulos et al. [30] conducted experiments and numerical models to study the efficiency of using ultra high-performance FRC for strengthening RC beams. Superior performance was obtained for strengthened RC beams, in which the largest ultimate moment was

increased by 178%. The findings of those studies demonstrated that the load-bearing capacity of the retrofitted and strengthened structures was enhanced. Nevertheless, they mostly focused on the repair and strengthening of RC structures without consideration of corrosion effects.

So far, very few studies have quantified the improvement of corroded RC structures retrofitted with high-performance fiber reinforced concrete/mortar (HPFRC/M). Meda et al. [31] presented a retrofitting technique for corroded RC columns using the HPFRC jacket. The experimental results demonstrated that the maximum load was increased by 118% and 65% compared to those of the corroded and non-corroded columns, respectively. Recently, Di Carlo et al. [32] developed numerical models to assess the cyclic behavior of corroded RC columns strengthened with external HPFRC jackets. Due to their high tensile strength, HPFRC jackets have positive influences on the confinement and global behavior of the columns. Aforesaid studies were mostly focusing on RC columns, a quantification of improvement of corroded RC beams after strengthening using HPFRC/M was not systematically investigated.

The purpose of this paper is to evaluate the flexural improvement of strength and ductility of corroded RC beams strengthened with high-performance steel fiber mortar. For this, six RC beams were imposed on corroded in 1 month, 2 months, and 3 months with a 3% NaCl solution and the direct current power type of $900 \mu\text{A}/\text{cm}^2$. Consequently, the reduction of reinforcing bar diameter of the beams due to three corrosion levels was 11.3%, 14.3%, and 24.8%, respectively. Those corroded RC beams are then strengthened using the high-performance steel fiber mortar jacket. The load–deflection relationships and crack evolutions were carefully observed. Moreover, a comparison of structural capacity between strengthened and non-strengthened RC beams was presented in this study.

2 Experimental Tests

2.1 Preparation of RC Beams

In this study, six identical simply supported RC beams, as shown in Fig. 1, were fabricated. The beam length was 3.3 m, in which the length between two supports was set to 3.0 m. The height and width of the cross-section were 300 mm and 200 mm, respectively. Two D16 reinforcing bars were arranged in the tensile area. Meanwhile, two D12 rebars were installed in the compression area. Transversal reinforcements (D6) with 150 mm spacing were used. The mechanical properties, shown in Table 1, were obtained from the laboratory tests of used reinforcements. All values in the table were averaged of three specimens for each

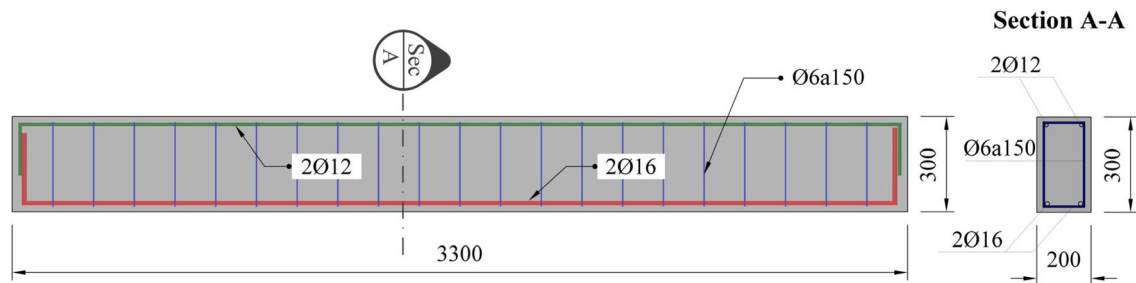


Fig. 1 Dimensions and reinforcement details of RC beams

Table 1 Properties of reinforcing bars

Diameter	Yield strength, f_y (MPa)	Ultimate strength, f_u (MPa)	Elastic modulus, E_s (GPa)	Area (mm ²)
D6	378.5	543	200	28.27
D12	364.1	508.7	200	78.54
D16	353.4	499.4	200	314.2

Table 2 Concrete proportions

Water, W (lit)	Cement, C (kg)	W/C	Sand (kg)	Stone (kg)	Slump (mm)	Strength, f'_c (MPa) (28 days)
188	328	0.573	594	1123	60	26.3

reinforcing bar. All the beams, after construction, were cured under laboratory conditions for 28 days. Six RC beams were divided into three pairs, which are corroded with various corrosion levels including 1 month, 2 months, and 3 months. After conducting the accelerated corrosion, three different corroded beams (referred as C1, C2, and C3) were taken for bending tests. In the meantime, the three remaining beams (referred as H1, H2, H3) were removed concrete cover and thereafter strengthened with high-strength steel fiber mortar and reinforcements. Additionally, a non-corroded RC beam (referred as DC), which was tested previously by authors, was used as a reference in this study.

The concrete mix was designed for obtaining a compressive strength (f'_c) of 25 MPa. Coarse aggregate with rock type 1 × 2 is usually used for normal concrete. Therefore, macadam has the largest particle size of 20 mm. Meanwhile, sand with a fineness modulus of 2.4 was used. The designed slump of the concrete was set to 10 ± 2 cm. The proportion of concrete mix is described in Table 2. The procedure for the fabrication of RC beams is shown in Fig. 2.

2.2 Corrosion Tests

A range of 3–5% NaCl solution and 100–3000 $\mu\text{A}/\text{cm}^2$ electrical current density have been widely used in conducting the accelerated corrosion process [33–36]. In this study, to speed up the corrosion of the reinforcement, the RC beams were immersed in a salt 3% NaCl solution, and the reinforcing bars were connected to a direct current of 900 $\mu\text{A}/\text{cm}^2$. The three pairs of RC beams were corroded in 1 month, 2 months, and 3 months, respectively. According to the design of the corrosion test, reinforcements were connected to the current anode, while the negative electrode of the current was connected to a copper rod. The use of power supply DC QJ6030S (0 ~ 60 V / 0 ~ 30A, 2 Output) for testing is shown in Fig. 3.

The electric current was adjusted so that the calculated intensity runs through each beam of 900 $\mu\text{A}/\text{cm}^2$. The adjustment was based on the cross-sectional area of the reinforcement. An empirical relationship between the corrosion time and the percentage of weight loss of reinforcement is given by Eq. (1), which was proposed by Tran [37] based on experiments. Accordingly, the times for three corrosion test levels, which are corresponding to the weight

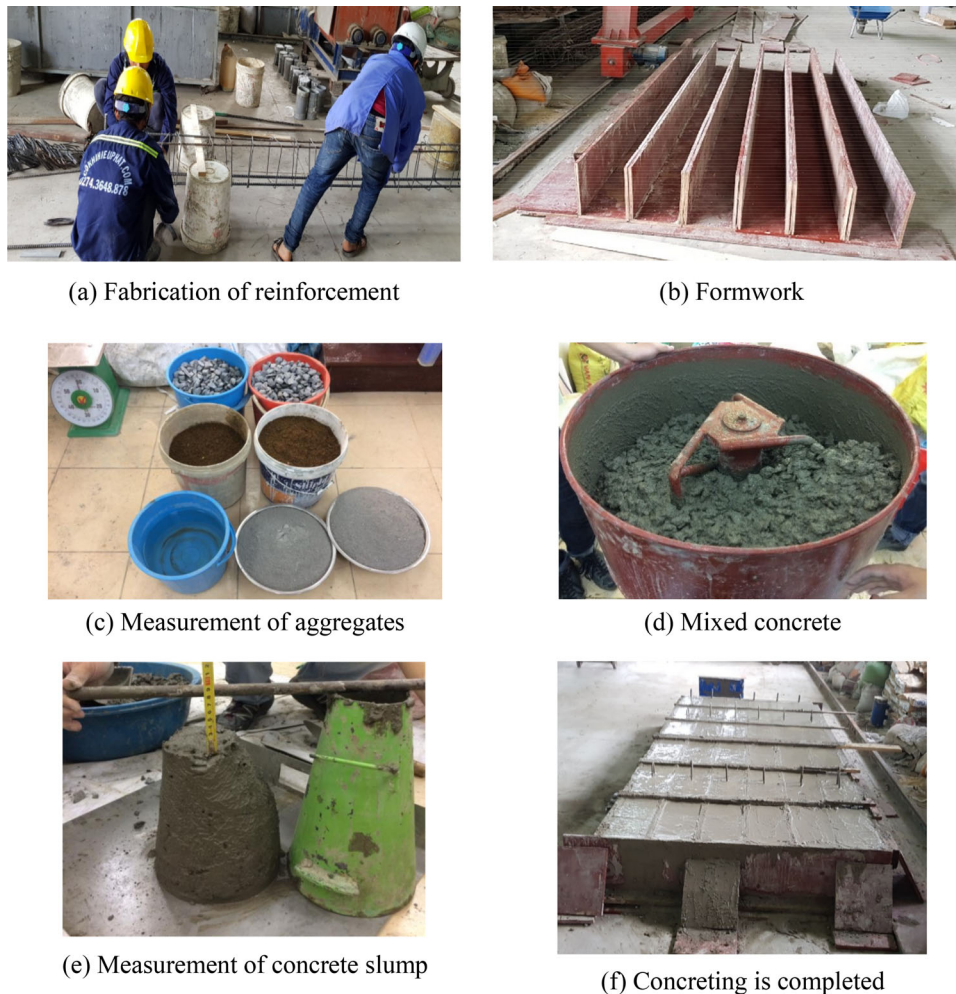


Fig. 2 Fabrication of RC beams

loss of reinforcement 7%, 14%, and 21%, are shown in Table 3.

$$\begin{aligned} W &= 0.235I.t \quad \text{for } I.t < 66 \text{ A.hr} \\ W &= 0.617I.t - 25.305 \quad \text{for } I.t > 66 \text{ A.hr} \end{aligned} \quad (1)$$

where W is the weight loss of reinforcement (g), t is the corrosion time (hr), I is the electric current intensity ($I = 3.618 \text{ A}$).

All RC beams were immersed in a test tank with a solution of electrolysis. The beams were corroded with the 3% NaCl solution, as shown in Fig. 4a. To maintain the salt content in the tank, experiments were regularly monitored, tested, and maintained to ensure a stable operation. After 7 days of testing, the steel rebar surface appeared reddish rust in the position adjacent to the water level. After 30 days, the steel rebars were connected to the source also appeared scaly rust scales 0.5–1 mm, as shown in Fig. 4b.

After finishing the corrosion process, cracks appeared on the concrete surface of the beams at some locations, as

shown in Fig. 4c. Cracks were concentrated on the areas, where the reinforcements were located. This observation is because the corrosive product compounds increased the volume of the reinforcements, then created pressure acting on the concrete area around the reinforcements. Due to the volumetric expansion, the stress in the concrete was increased and cracks were appeared in the concrete surface. The deterioration of concrete structures is usually divided into three main stages, as follows.

- The initial stage is defined as the time from the onset of corrosion to the reinforcement until the corrosion of the reinforcement causes the initial cracks in the concrete.
- The propagation stage and accelerating stage are determined when the crack propagates and binds together when the amount of reinforcement corrosion.
- The failure stage is defined when the cracks getting large and strain causes the peeling or spalling of the concrete cover. During this stage, corrosion causes

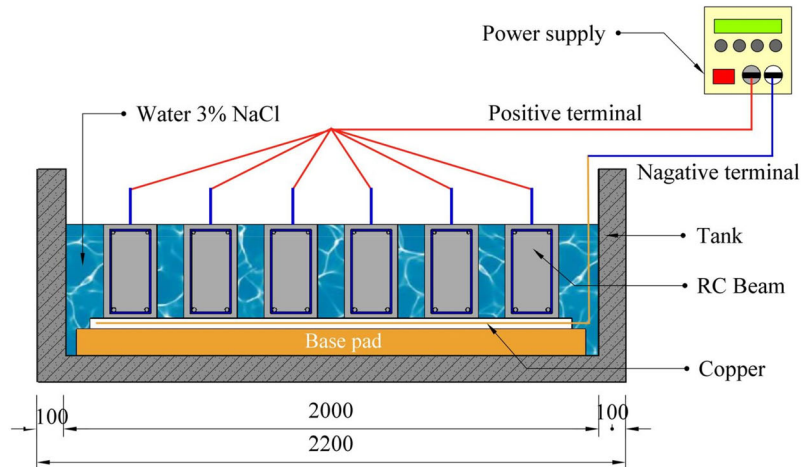
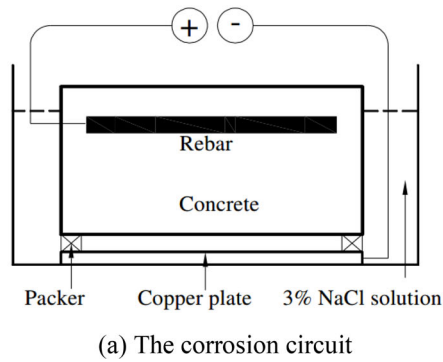


Fig. 3 The accelerated corrosion test

Table 3 Time to stop the corrosion test for reinforcement

RC beam	Weight loss of steel, (%)	Weight loss of steel, W (g)	Time, t (hr)
C1 and H1	7	1582	720
C2 and H2	14	3189	1440
C3 and H3	21	4796	2160

cracks that significantly impair the bearing capacity and the service life of the concrete structure.

2.3 Strengthening of Corroded RC Beams with High-Performance Steel Fiber Mortar

After accelerating corrosion tests, three beams with three corrosion levels (1 month, 2 months, and 3 months) were selected to strengthen with high-performance steel fiber mortar. Figure 5 shows the dimensions of the beam before and after strengthening with high-strength steel fiber mortar and reinforcements. It should be noted that the concrete cover was removed within two thirds of the beam depth

and the bottom, as cross-hatched in Fig. 5. These beams are referred, namely, H1, H2, and H3. The ratio of water to cement was 0.325. In this mortar mix, black silica fume with 15% of the weight of cement, was used, as shown in Fig. 6a. The BASF ACE 8588 superplasticizer was used with 2% of the weight of cement. Steel fibers (in Fig. 6b) with a tensile strength of 2985 MPa, provided by Anhui Elite Industrial Co., Ltd. [38], was utilized for strengthening. The fiber length and diameter are 0.2 mm and 12.8 mm, respectively.

To avoid clumping of the reinforcement, the reinforcement was sprinkled into the mortar mixture during the mixing process through a plastic rack, as shown in Fig. 6c,

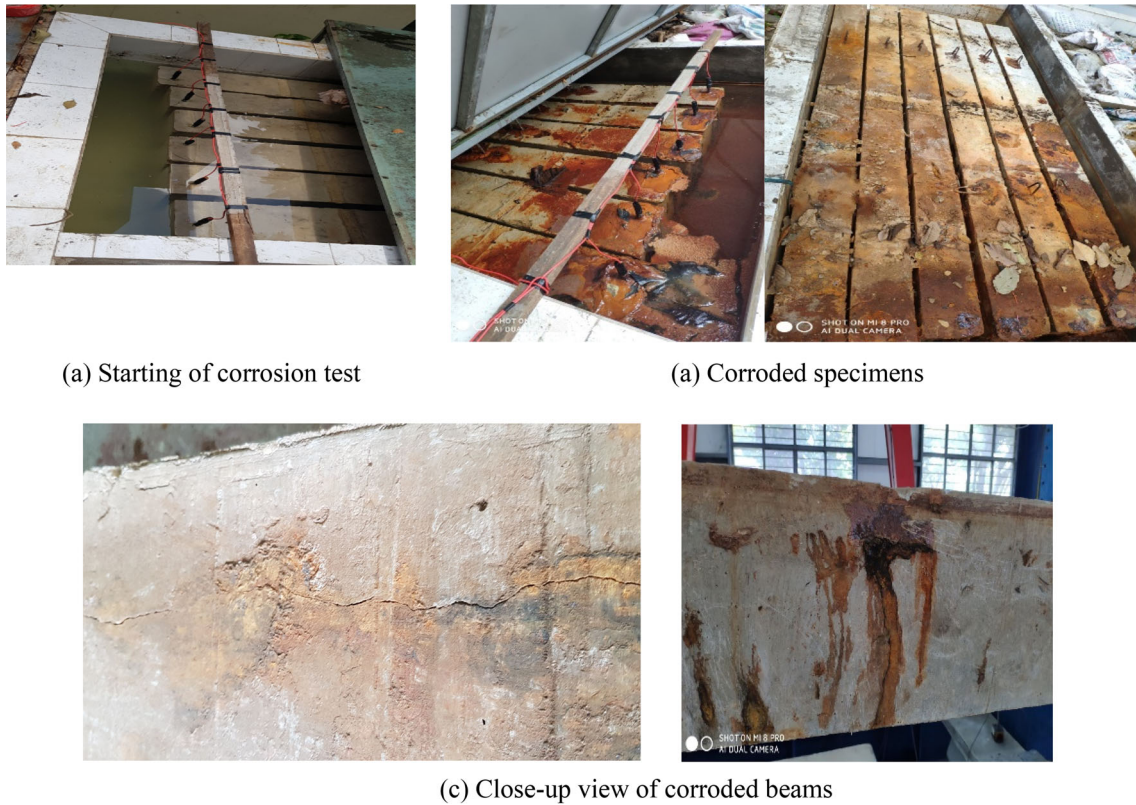


Fig. 4 RC beams during accelerated corrosion tests

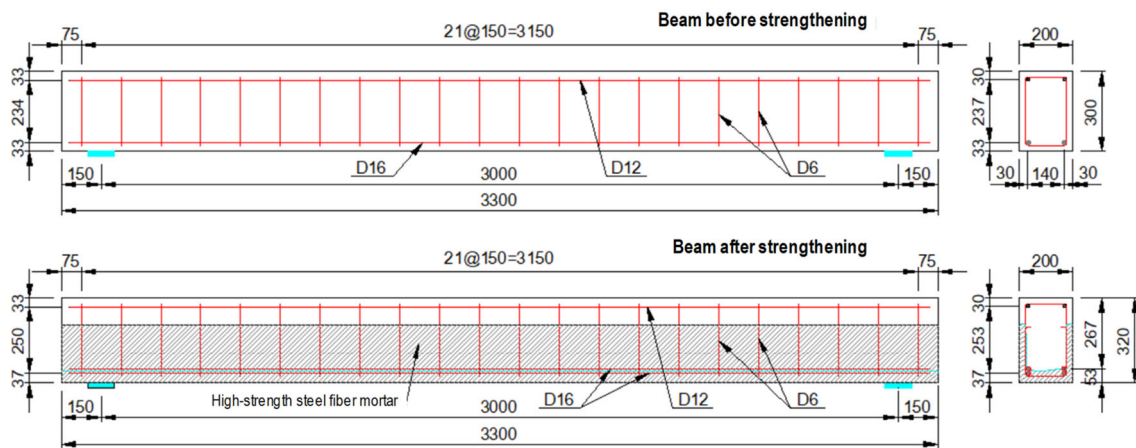


Fig. 5 Configuration of RC beams before and after strengthening

to increase evenly dispersion. The mortar gradation determined for a single pour was 60 lits, as shown in Table 4. It should be noted that a forced mixer with a capacity of 80 lits was used to mix concrete and high strength fibers. For testing the high-performance steel fiber mortar, the cylindrical mold with a diameter of 5 cm and a height of 10 cm was performed. The sand used in the high-performance steel fiber mortar was washed and dried to constant mass before pouring, and its fineness modulus determined

according to ASTM C125 [39] was 3.05. The density measured in a pycnometer as per ASTM C128 [40] was 2.67 ton/m^3 . The water absorption of sand tested according to ASTM C128 was 1.6%. The amount of water desiccant of the sand must be considered during the experiment. Figure 6d shows the mixed high-performance steel fiber mortar for the strengthening of the corroded RC beams.

The beams H1, H2, and H3 were taken from the corrosion test and removed the cover concrete, as shown in

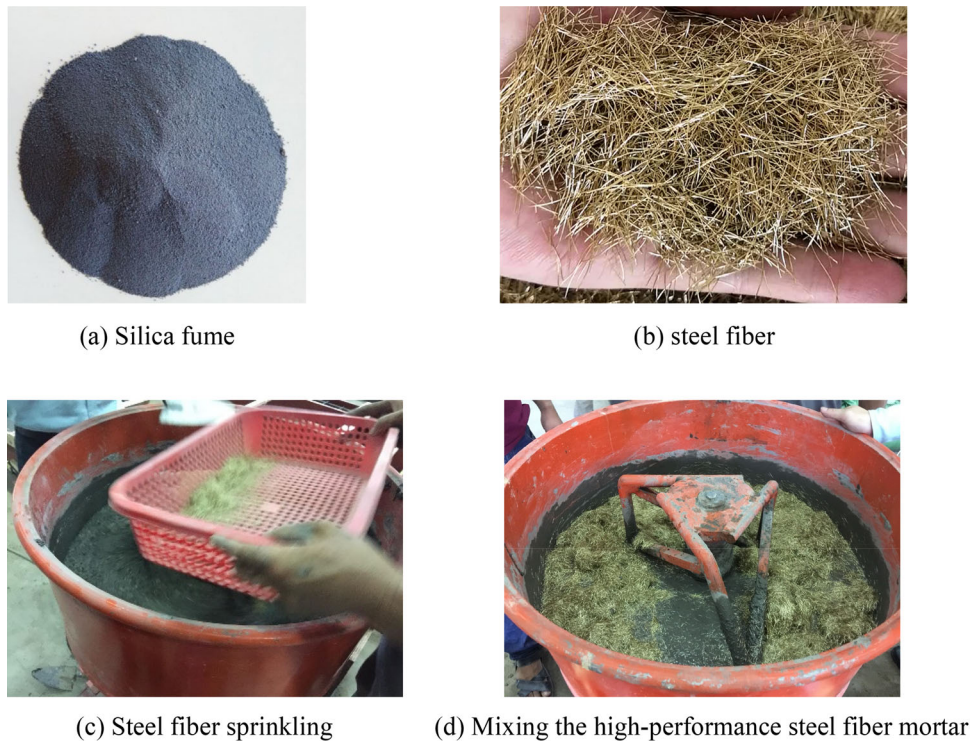


Fig. 6 High-performance steel fiber mortar

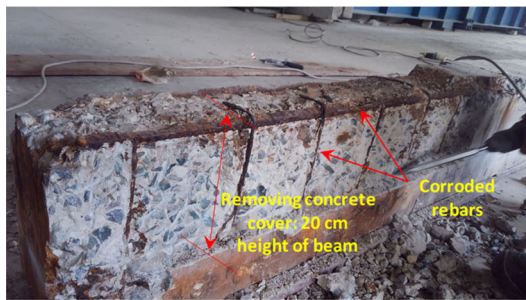
Table 4 High-performance fiber steel mortar proportions

W/C	Water, W (l)	Cement, C (kg)	Sand, (kg)	Silica fume (kg)	Additives (kg)	Micro steel fiber (kg)	Slump (mm)	Strength, f'_c (MPa)
0.325	14.7	40	83.1	6.0	0.8	4.48	240	72.6

Fig. 7a. All cover concrete layer at two thirds of the beam height (i.e., 20 cm) and the bottom were removed using concrete cutters and drills, as shown in Fig. 7a–b. The reinforcements were cleaned of the corroded part and continue to use. Two longitudinal reinforcements with D16 were newly added to the tensile area, as shown in Fig. 7b. The new bars were connected to the old bars (i.e., corroded ones) using binding wires, as shown in Fig. 7c. Additionally, U-shaped transversal reinforcements (in Fig. 7d) with a diameter of 6 mm and a spacing of 150 mm were attached to the beams. The new transversal rebars were drilled into the concrete and binned with the longitudinal rebars using steel wires. After setting up the formwork (Fig. 7e), self-compacting high-performance steel fiber mortar was poured to strengthen the corroded RC beams as well as provide a protective layer for the reinforcements (Fig. 7f). Therefore, the cross-sectional height of the beam after strengthening was increased up to 320 mm, as shown in Fig. 7g.

2.4 Bending Tests of RC Beams

All three corroded RC beams and three strengthened RC beams with high-performance steel fiber were then taken to bending tests. The test set-up is illustrated in Fig. 8. The RC beams were placed on two bearings and loaded through two points, as shown in Fig. 9. The applied load was gradually increased through the beam deflection control. The loader and strain gauges were connected to the data logger so that the force and deflection can be recorded simultaneously. Additionally, two pi-gauges were used to detect cracks occurring on the beam. One is at the center of the beam and the other is on the left of the beam. During the loading process, the relationship between applied load and deflection as well as crack formations were monitored.



(a) Removing concrete cover



(b) Installing strengthening reinforcing bars



(c) Attachment of new reinforcements



(d) Additional U-shaped rebars



(e) Installing the formworks



(f) Pouring the high-performance steel fiber mortar



(g) Removing the formworks

Fig. 7 Strengthening of corroded RC beams using high-performance steel fiber mortar

3 Results and Discussion

3.1 Weight Reduction of Reinforcing Bars after Corrosion

The tested beams were crushed to remove the reinforcing bars and the diameter of all rebars was measured, as shown in Fig. 10a. Then, the weight of the remaining rebars was

checked, as shown in Fig. 10b. Noting that, in this figure, the DC is referred to as the non-corroded RC beam, while H1, H2, and H3 are referred to as 1-month, 2-month, and 3-month corroded RC beams. For the DC beam, the original weight of reinforcements was 23 kg, whereas, the weight of beams H1, H2, and H3 was reduced to 20.4 kg, 19.7 kg, and 17.3 kg, respectively. In other words, the weight loss of those corroded beams was 11.3%, 14.3%,

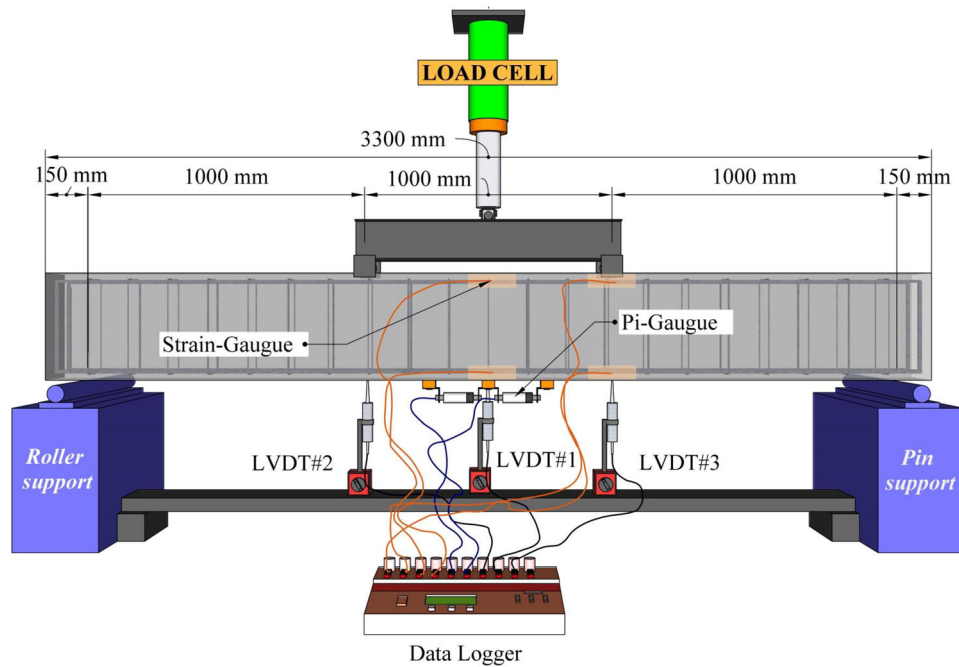


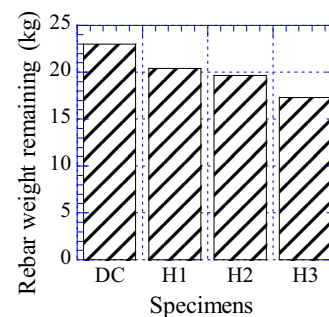
Fig. 8 Schematic diagram of experiments



Fig. 9 Bending test setup



(a) Measuring diameter of rebar after corrosion



(b) Weight of rebars after corrosion

Fig. 10 Weight reduction of reinforcing bars after corrosion

and 24.8%, respectively. The longer embedded time in the salt solution the more corroded in the RC beam. Moreover, the loss of reinforcement due to corrosion was not even along with the reinforcing bars. Accordingly, the cracks were spread wider at where the reinforcement was

corroded. The experimental result showed that the corrosion of reinforcement was mostly focused on the middle area of RC beams. The observed result can be attributed to the reason that the middle area contains a higher moment under its self-weight, therefore few micro cracks have

occurred in the area leading to higher corrosion during the accelerated corrosion procedure [41].

It should be noted that since the beams in each pair are identical, the weight loss of reinforcement was assumed to be mostly identical. Specifically, the weight loss of steel values was measured after demolition of C1, C2, and C3.

3.2 Load–Displacement Relationship

Figure 11 shows the relationship between load and deflection of different tested RC beams including three various corroded beams (i.e., C1, C2, and C3), three strengthened beams with high-performance steel fiber mortar and normal reinforcements (i.e., H1, H2, and H3), and one non-corroded beam (i.e., DC). It can be observed that the flexural stiffness and ductility of beams strengthened with high-performance steel fiber mortar and normal reinforcements were significantly improved than those of the corroded and non-corroded beams. Moreover, there was a minor difference in strength and stiffness of the

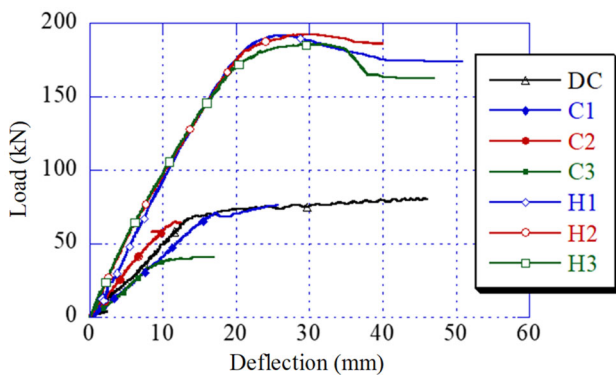


Fig. 11 Load versus displacement at the middle of the tested beams

corroded RC beams after strengthening. It is attributed to the reason that the high-performance steel fiber mortar plays a very important role in providing the flexural capacity of the RC beam.

The strength of beams H1, H2, and H3 were 191.87 kN, 192.37 kN, and 185.94 kN, respectively, with a difference of less than 3.3%. The mean strength of those strengthened beams was 190.06 kN, which was 2.35 times higher than that of the non-corroded beam (i.e., 80.91 kN). After strengthening, the strength of the beams was 2.52 times increased than that of the corroded beams (i.e., C1, C2, and C3).

Additionally, the stiffness and ductility of strengthened RC beams were significantly improved compared to those of corroded beams. The stiffness of retrofitting beams was double increased than that of non-retrofitted beams, meanwhile, the ductility was 1.5–2.0 times enhanced after strengthening. Also, a descending branch was visible in the load–deflection curves of the strengthening RC beams. This behavior was not observed for the non-retrofitted beams, which was failure suddenly after reaching a yielding state. This finding highlighted that the high-performance steel fiber mortar can be a feasible solution for the strengthening of corroded or degraded RC structures.

Figure 12 shows the relationship between applied load and strain of concrete at the middle of the strengthened beams. It can be found that the tensile concrete strains of strengthened beams H1, H2, and H3 were rapidly developed after the applied loads exceeded 100 kN, 70 kN, and 50 kN, respectively. Additionally, at a load of 185 kN, all the beams reached tensile strains, approximately, 3200, 3500, and 4000 mm/mm, respectively. Meanwhile, the compressive concrete strains of those beams were gradually increased up to ultimate values, 2300, 2100, and 2000 mm/mm, respectively.

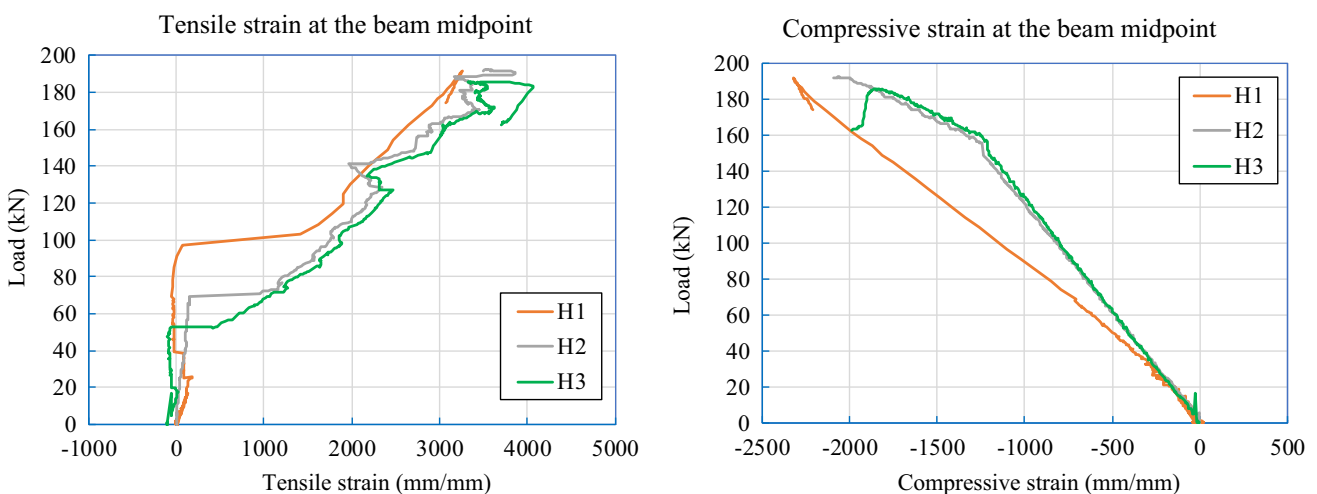


Fig. 12 Load versus strain of concrete at the middle of strengthened beams

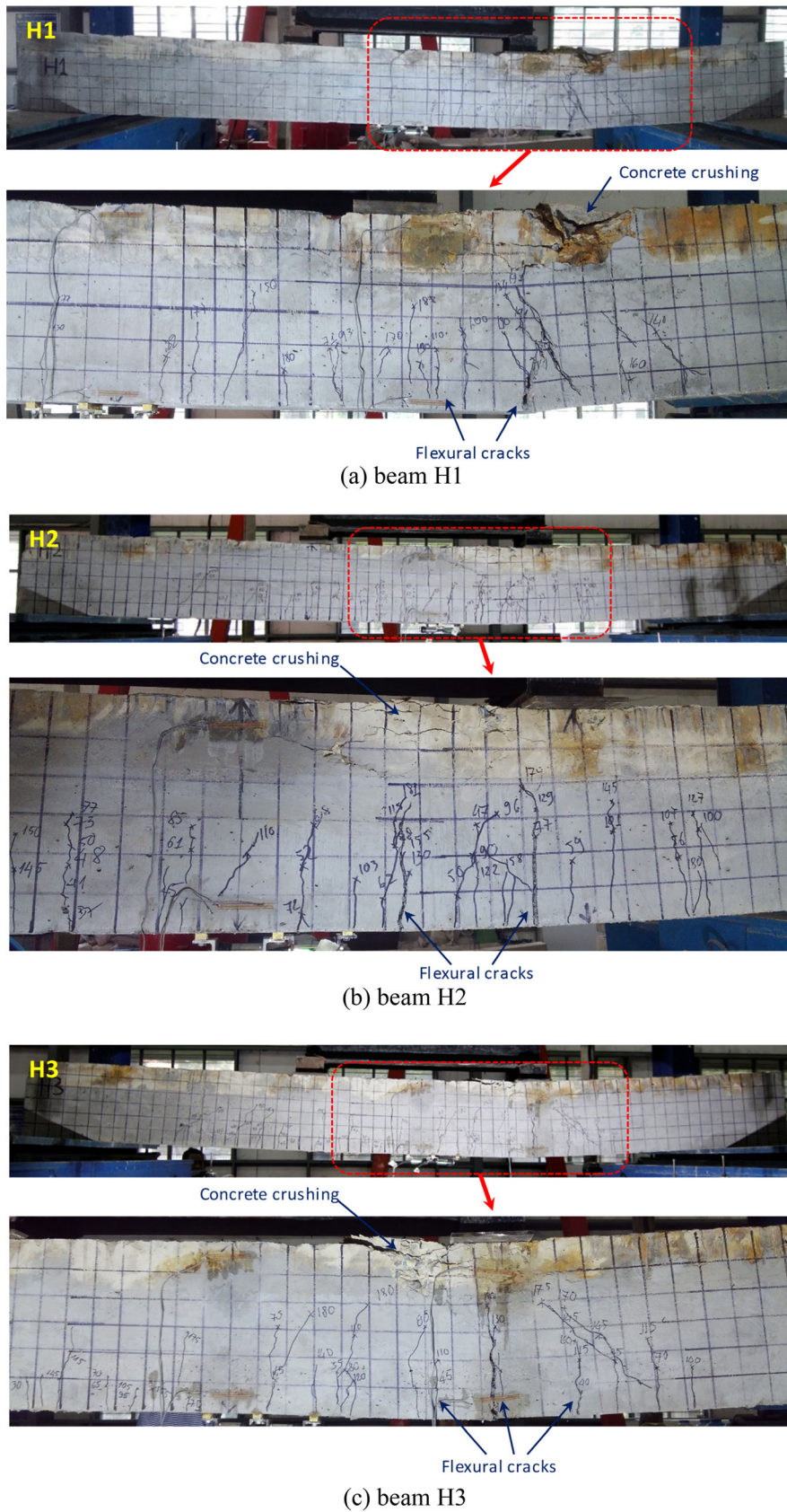


Fig. 13 Crack distribution of the strengthened beams

3.3 Crack Development

Crack patterns of strengthened beams are shown in Fig. 13. The space of these cracks is relatively even. For beam H1, cracks were formed at the middle beam with the load of 32 kN, then was spread further to other regions. At the load of 116 kN, the width of the crack was 0.1 mm at the middle beam. When the load was increased up to 150 kN, the cracks were more developed. At this time, the crack under the load point on the right was significantly opened, then inclined toward the load point. Also, adjacent cracks were continuously developed. At the applied load of 191.87 kN, the cracks were significantly developed, the beam reached ultimate capacity. Finally, the beam was failed in flexure. It can be attributed to the reason that the tensile stress was focused on the middle area of the beams. As the applied load increased, the tensile stress was increased, and the flexural cracks occurred when the demand exceeded the capacity. These failure modes were observed for both three strengthened RC beams.

Regarding beam H2, the first crack occurred at the middle beam with the load of 37 kN, then it was spread to both sides. At the load of 104 kN, the crack width was 0.1 mm at the middle beam. Similar to beam H1, at the

load up to 145 kN, the cracks were more developed toward the compressive zone and significantly opened. Then, the load was increased to 192.37 kN, the beam was attained the ultimate strength and started losing capacity.

Similarly, the first crack occurred at the middle of beam H3 with a load of 30 kN, then the crack was spread out to nearby regions. At the load up to 130 kN, the cracks under load points were more developed toward the compressive zone and significantly opened. The development of cracks on beams H2 and H3 was quite similar. Since the applied load was increased up to 192.37 kN, the beam was attained the ultimate strength and it started losing capacity.

Figure 14 shows the evolution of crack width at the middle of strengthened beams. The crack widths of H1, H2, and H3 were gradually expanded and attained the ultimate values of 0.15, 0.23, and 0.22 mm, respectively. Moreover, it was shown that the crack width of beams H2 and H3 were larger than that of H1. This is attributed to the reason that beam H2 and H3 were more significantly corroded than that H1 was imposed.

4 Comparison Between Theory and Experiment Results

In this section, a comparison of the flexural capacity of RC beam between theory and experimental tests is presented to emphasize the contribution of high-performance steel fiber mortar to flexural strength. The theoretical calculation of the flexural capacity of RC beams is shown in Fig. 15. The results of the calculated theory were complied with the guideline of TCVN 5574-2012, as provided in Table 5. It was found that bending moments (i.e., M_u) of three beams H1, H2, and H3 without strengthening with high-performance mortar were 68.1, 66.8, and 63.4 kN.m, respectively. Specifically, the bending moments of the H2 beam and H3 beam were relatively smaller than that of H1 since the reinforcement loss in H2 and H3 beams was higher than that in H1. Accordingly, the calculated ultimate loading ($P_u^{cal.}$) can be determined using equation $P_u^{cal.} = 6M_u/L$, resulted as 136.2, 133.7, and 126.8 kN, respectively. It should be noted that the theoretical calculation ignored the

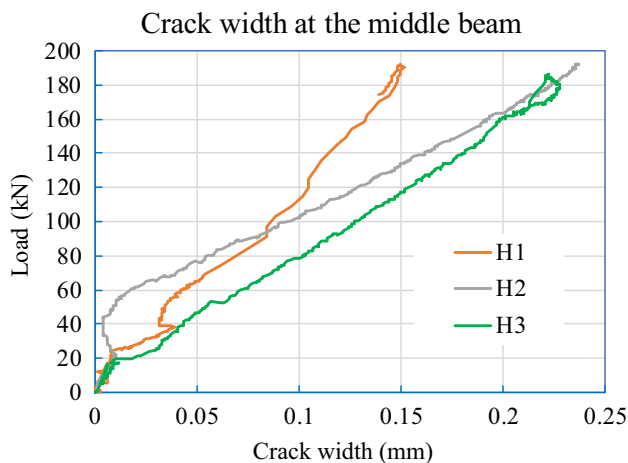


Fig. 14 Development of crack width at the middle of strengthened beams

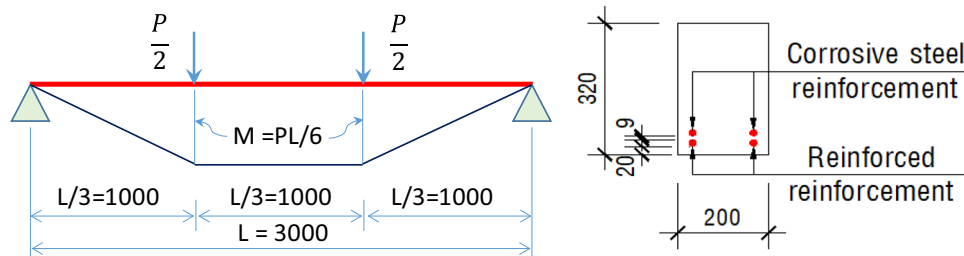


Fig. 15 Calculation of flexural capacity of RC beam

Table 5 Results of calculated theory and experiments

Beam	Weight loss of steel (%)	f'_c (MPa)	h (mm)	b (mm)	A'_s (mm ²)	A_s (mm ²)	M_u (kN.m)	$P_u^{cal.}$ (kN)	$P_u^{exp.}$ (kN)	$\frac{P_u^{exp.}}{P_u^{cal.}}$
DC	0	26.3	300	200	262.2	402.2	36.000	72.00	80.91	1.12
H1	11.30	19.4	320	200	262.2	759.0	68.125	136.25	191.87	1.40
H2	14.30	17.2	320	200	262.2	746.9	66.884	133.77	192.37	1.43
H3	24.80	16.6	320	200	262.2	704.7	63.402	126.80	185.94	1.46

tensile strength of concrete and steel fiber mortar. In other words, the $P_u^{cal.}$ values in Table 5 do not consider the effects of the steel fiber mortar.

Based on experimental tests, the load corresponding to the ultimate strength of the beams was obtained, as presented in Sect. 3.2. The experiment-based ultimate loading results of H1, H2, and H3, (i.e., $P_u^{exp.}$) were 191.8, 192.3, and 185.9 kN. It can be observed from Table 5 that after strengthening with the high-performance steel fiber mortar, the flexural resistance of the H1, H2, and H3 beams was increased by approximately 41%, 43%, and 46%, respectively, compared to those of non-retrofitted beams (i.e., without high-performance mortar). This finding highlighted that the high-performance steel fiber mortar had significant effects on the bearing capacity of the beam, even though reinforcing bars were newly added to the tensile region of RC beams. The difference between the experiment and calculation was contributed by the tensile strength of the high-strength steel fiber mortar.

5 Conclusions

Six reinforced concrete (RC) beams were corroded in 1 month, 2 months, and 3 months with a 3% NaCl solution and the direct current power type of 900 $\mu\text{A}/\text{cm}^2$. Those corroded beams were then strengthened using the high-performance steel fiber mortar and normal reinforcements. Flexural tests were conducted to evaluate the structural capacity improvement of strengthened RC beams. Based on experimental results, the following conclusions are drawn.

- The lost weights of reinforcement of RC beams due to 1-month, 2-month, and 3-month corrosion time are 11.3%, 14.3%, and 24.8%, respectively.
- The strength of retrofitted RC beams is increased by 2.35 and 2.52 times than that of non-corroded and corroded beams, respectively.
- After strengthening with high-performance steel fiber mortar, the flexural resistance of the strengthened RC beams H1, H2, and H3 were increased by 41%, 43%,

and 46%, respectively, compared to those of non-retrofitted beams.

- The stiffness and ductility of strengthened RC beams are significantly improved.
- High-performance steel fiber mortar can be a promising solution for the strengthening of corroded or degraded RC structures.

Acknowledgements The authors are grateful for the financial support of the project in 2022 funded by Ho Chi Minh City University of Technology and Education, Vietnam.

Funding This work belongs to the project in 2022 funded by Ho Chi Minh City University of Technology and Education, Vietnam.

Declarations

Conflict of interest The authors declare that they have no potential conflicts of interest in this paper.

References

1. Shi X, Xie N, Fortune K, Gong J (2012) Durability of steel reinforced concrete in chloride environments: an overview. *Constr Build Mater* 30:125–138
2. Abdel-Hay AS, Fawzy YAG (2015) Behavior of partially defected RC columns strengthened using steel jackets. *HBRC J* 11(2):194–200
3. Jiang CJ, Lu ZD, Li LZ (2017) Shear performance of fire-damaged reinforced concrete beams repaired by a bolted side-plating technique. *J Struct Eng* 143(5):04017007
4. Yang SH, Cao SY, Gu RN (2015) New technique for strengthening reinforced concrete beams with composite bonding steel plates. *Steel Compos Struct* 19(3):735–757
5. Sharif A, Al-Sulaimani GJ, Basunbul IA, Baluch MH, Husain M (1995) Strengthening of shear-damaged RC beams by external bonding of steel plates. *Mag Concr Res* 47(173):329–334
6. Vadoros KG, Dritsos SE (2008) Concrete jacket construction detail effectiveness when strengthening RC columns. *Constr Build Mater* 22(3):264–276
7. Campione G, Fossetti M, Giacchino C, Minafò G (2014) RC columns externally strengthened with RC jackets. *Mater Struct* 47(10):1715–1728
8. Alhadid MMA, Youssef MA (2017) Analysis of reinforced concrete beams strengthened using concrete jackets. *Eng Struct* 132:172–187
9. Al-Salloum YA, Elsanadedy HM, Alsayed SH, Iqbal RA (2012) Experimental and numerical study for the shear strengthening of

- reinforced concrete beams using textile-reinforced mortar. *J Compos Constr* 16(1):74–90
10. Escrig C, Gil L, Bernat-Maso E, Puigvert F (2015) Experimental and analytical study of reinforced concrete beams shear strengthened with different types of textile-reinforced mortar. *Constr Build Mater* 83:248–260
 11. Raouf SM, Koutas LN, Bournas DA (2017) Textile-reinforced mortar (TRM) versus fibre-reinforced polymers (FRP) in flexural strengthening of RC beams. *Constr Build Mater* 151:279–291
 12. Triantafyllou TC, Papanicolaou CG (2006) Shear strengthening of reinforced concrete members with textile reinforced mortar (TRM) jackets. *Mater Struct* 39(1):93–103
 13. Siddika A, Al Mamun MA, Alyousef R, Amran YM (2019) Strengthening of reinforced concrete beams by using fiber-reinforced polymer composites: a review. *J Build Eng*. <https://doi.org/10.1016/j.jobbe.2019.100798>
 14. Grace NF, Sayed GA, Soliman AK, Saleh KR (1999) Strengthening reinforced concrete beams using fiber reinforced polymer (FRP) laminates. *ACI Struct J Am Concr Inst* 96(5):865–874
 15. Gonzalez-Libreros JH, Sneed LH, D'Antino T, Pellegrino C (2017) Behavior of RC beams strengthened in shear with FRP and FRCM composites. *Eng Struct* 150:830–842
 16. Zhang SS, Ke Y, Smith ST, Zhu HP, Wang ZL (2021) Effect of FRP U-jackets on the behaviour of RC beams strengthened in flexure with NSM CFRP strips. *Compos Struct*. <https://doi.org/10.1016/j.compstruct.2020.113095>
 17. El Maaddawy T, Soudki K (2005) Carbon-fiber-reinforced polymer repair to extend service life of corroded reinforced concrete beams. *J Compos Constr* 9(2):187–194
 18. Al-Saidy AH, Al-Harthy AS, Al-Jabri KS, Abdul-Halim M, Al-Shidi NM (2010) Structural performance of corroded RC beams repaired with CFRP sheets. *Compos Struct* 92(8):1931–1938
 19. Triantafyllou GG, Rousakis TC, Karabinis AI (2017) Corroded RC beams patch repaired and strengthened in flexure with fiber-reinforced polymer laminates. *Compos B Eng* 112:125–136
 20. Sevil T, Baran M, Bilir T, Canbay E (2011) Use of steel fiber reinforced mortar for seismic strengthening. *Constr Build Mater* 25(2):892–899
 21. Shah SP, Naaman AE (1976) Mechanical properties of glass and steel fiber reinforced mortar. *ACI J Proc* 73(1):50–53
 22. Iqbal S, Ali A, Holschemacher K, Bier TA, Shah AA (2016) Strengthening of RC beams using steel fiber reinforced high strength lightweight self-compacting concrete (SHLSCC) and their strength predictions. *Mater Des* 100:37–46
 23. Mohammed TJ, Bakar BA, Bunnori NM (2016) Torsional improvement of reinforced concrete beams using ultra high-performance fiber reinforced concrete (UHPFC) jackets—experimental study. *Constr Build Mater* 106:533–542
 24. Gonzalez-Libreros JH, Sabau C, Sneed LH, Pellegrino C, Sas G (2017) State of research on shear strengthening of RC beams with FRCM composites. *Constr Build Mater* 149:444–458
 25. Simoncello N, Zampieri P, Gonzalez-Libreros J, Pellegrino C (2019) Experimental behaviour of damaged masonry arches strengthened with steel fiber reinforced mortar (SFRM). *Compos B Eng*. <https://doi.org/10.1016/j.compositesb.2019.107386>
 26. Attar HS, Esfahani MR, Ramezani A (2020) Experimental investigation of flexural and shear strengthening of RC beams using fiber-reinforced self-consolidating concrete jackets. *Structures* 27:46–53
 27. Maraq MAA, Tayeh BA, Ziara MM, Alyousef R (2021) Flexural behavior of RC beams strengthened with steel wire mesh and self-compacting concrete jacketing—experimental investigation and test results. *J Mater Res Technol* 10:1002–1019
 28. Martinola G, Meda A, Plizzari GA, Rinaldi Z (2010) Strengthening and repair of RC beams with fiber reinforced concrete. *Cem Concr Compos* 32(9):731–739
 29. Ruano G, Isla F, Pedraza RI, Sfer D, Luccioni B (2014) Shear retrofitting of reinforced concrete beams with steel fiber reinforced concrete. *Constr Build Mater* 54:646–658
 30. Lampropoulos AP, Paschalis SA, Tsioulou OT, Dritsos SE (2016) Strengthening of reinforced concrete beams using ultra high performance fibre reinforced concrete (UHPFRC). *Eng Struct* 106:370–384
 31. Meda A, Mostosi S, Rinaldi Z, Riva P (2016) Corroded RC columns repair and strengthening with high performance fiber reinforced concrete jacket. *Mater Struct* 49(5):1967–1978
 32. Di Carlo F, Meda A, Rinaldi Z (2017) Numerical cyclic behaviour of un-corroded and corroded RC columns reinforced with HPFRC jacket. *Compos Struct* 163:432–443
 33. El Maaddawy TA, Soudki KA (2003) Effectiveness of impressed current technique to simulate corrosion of steel reinforcement in concrete. *J Mater Civ Eng* 15(1):41–47
 34. Rodriguez J, Ortega LM, Casal J (1997) Load carrying capacity of concrete structures with corroded reinforcement. *Constr Build Mater* 11(4):239–248
 35. Zhu W, François R, Coronelli D, Cleland D (2013) Effect of corrosion of reinforcement on the mechanical behaviour of highly corroded RC beams. *Eng Struct* 56:544–554
 36. Loreto G, Di Benedetti M, Iovino R, Nanni A, Gonzalez MA (2011) Evaluation of corrosion effect in reinforced concrete by chloride exposure. *Nondestructive characterization for composite materials, aerospace engineering, civil infrastructure, and homeland security 2011*, vol 7983. International Society for Optics and Photonics, p 79830A
 37. Tran KK (2012) Study on cracking behavior of concrete due to rebar corrosion. Doctor Thesis. Nagoya University, Japan
 38. Anhui Elite Industrial Co., Ltd., <https://www.ahelite.com/>
 39. ASTM International (2007) Standard terminology relating to concrete and concrete aggregates. ASTM C125, West Conshohocken, Pennsylvania, USA
 40. ASTM International (2007) Standard test method for density, relative density (specific gravity), and absorption of fine aggregate. ASTM C128, West Conshohocken, Pennsylvania, USA
 41. Ballim Y, Reid JC (2003) Reinforcement corrosion and the deflection of RC beams—an experimental critique of current test methods. *Cem Concr Compos* 25(6):625–632